AGU PUBLICATIONS

JGR

Journal of Geophysical Research: Biogeosciences

RESEARCH ARTICLE
10.1002/2013JG002350

Key Points:
- Aquifer biogeochemical processes are heterogeneously distributed
- The subsurface is generally in C metabolic balance
- Hotspots of organic matter mineralization and autotrophy are found

Supporting Information:
- Table S1
- Table S2
- Table S3
- Table S4
- Figure S1
- Figure S2
- Figure S3
- Figure S4

Correspondence to:
A. R. Zimmerman,
azimmer@ufl.edu

Citation:
Jin, J., A. R. Zimmerman, P. J. Moore, and J. B. Martin (2014), Organic and inorganic carbon dynamics in a karst aquifer: Santa Fe River Sink-Rise system, north Florida, USA, *J. Geophys. Res. Biogeosci.*, *119*, doi:10.1002/2013JG002350.

Received 27 MAR 2013
Accepted 9 FEB 2014
Accepted article online 14 FEB 2014

Organic and inorganic carbon dynamics in a karst aquifer: Santa Fe River Sink-Rise system, north Florida, USA

Jin Jin[1], Andrew R. Zimmerman[1], Paul J. Moore[1,2], and Jonathan B. Martin[1]

[1]Department of Geological Sciences, University of Florida, Gainesville, Florida, USA, [2]ExxonMobil Exploration Company, Houston, Texas, USA

Abstract Spatiotemporal variations in dissolved organic carbon (DOC), dissolved inorganic carbon (DIC), major ions concentrations and other geochemical parameters including stable carbon isotopes of DIC ($\delta^{13}C_{DIC}$), were measured in surface water and deep and shallow well water samples of the Santa Fe River Sink-Rise eogenetic karst system, north Florida, USA. Three end-member water sources were identified: one DOC-rich/DIC-poor/$\delta^{13}C_{DIC}$-depleted, one DOC-poor/DIC-rich/$\delta^{13}C_{DIC}$-enriched, and one enriched in major ions. Given their spatiotemporal distributions, they were presumed to represent soil water, upper aquifer groundwater, and deep aquifer water sources, respectively. Using assumed ratios of Na^+, Cl, and SO_4^{2-} for each end-member, a mixing model calculated the contribution of each water source to each sample. Then, chemical effects of biogeochemical reactions were calculated as the difference between those predicted by the mixing model and measured species concentrations. In general, carbonate mineral dissolution occurred throughout the Sink-Rise system, surface waters were net autotrophic and the subsurface was in metabolic balance, i.e., no net DOC or DIC production or consumption. However, there was evidence for chemolithoautotrophy, perhaps by hydrogen oxidizing microbes, at some deep aquifer sites. Mineralization of this autochthonous natural dissolved organic matter (NDOM) led to localized carbonate dissolution as did surface water-derived NDOM supplied to shallow well sites during the highest flow periods. This study demonstrates linkages between hydrology, abiotic and microbial processes and carbon dynamics and has important implications for groundwater quality, karst morphologic evolution, and hydrogeologic projects such as aquifer storage and recovery in karst systems.

1. Introduction

Karst aquifers are important geomorphic features as they cover 20% of the ice-free global land surface and provide 25% of human's drinking water supplies [*Ford and Williams*, 2007]. Because of their typically high permeability [*Worthington*, 1994], karst aquifers are hydrologically coupled to surface water and thus can receive surface-produced natural dissolved organic matter (NDOM) [*Lau and Mink*, 1987] and associated nutrients. Likewise, karst aquifers are susceptible to contaminants from the surface, whose fate and transport is largely controlled by the water-rock-microbe interactions in the subsurface. Karst areas may also be an important but overlooked part of the global carbon (C) cycle.

Karst aquifers can be divided into those with low matrix permeability (telogenetic) and those that retain high matrix permeability (eogenetic) [*Vacher and Mylroie*, 2002]. Flow in a telogenetic karst aquifer thus occurs mainly in conduits and fractures, whereas a large portion of flow in eogenetic karst aquifers occurs within the intergranular porosity of the matrix [*Martin and Dean*, 2001; *Screaton et al*., 2004]. Because flow occurs at different rates in each portion of eogenetic karst aquifers, biogeochemical reactions involving NDOM and other solutes are likely to vary within each portion as a function of the residence time and flux of solutes. Most well-studied karst aquifers are telogenetic [e.g., *Vacher and Mylroie*, 2002; *Ford and Williams*, 2007], while only a few studies [e.g., *Martin and Dean*, 2001; *Gulley et al*., 2011] have focused on eogenetic karst aquifers, although biogeochemical reactions could be more extensive in eogenetic karst aquifers because matrix flow in eogenetic systems plays a larger role in these systems. A good example of an eogenetic karst aquifer, and the site of this study, is the upper Floridan aquifer (UFA), which retains up to 20% intergranular matrix porosity [*Budd and Vacher*, 2004].

As a ubiquitous solute in all natural waters including karst system, NDOM is derived from the exudates and degradation products of microbes and plants and is complex and heterogeneous in nature, with a wide range of molecular masses and chemical structures [*Findlay and Sinsabaugh*, 2003; *Frimmel*, 1998]. Through its interaction with other aquifer components including rocks, metals, and microbes, NDOM plays an important role in controlling the biogeochemistry and hydrogeology in the subsurface. For example, NDOM can act as a proton donor or acceptor [*Frimmel*, 1998; *Jiang and Kappler*, 2008; *Ratasuk and Nanny*, 2007], influence mineral precipitation and dissolution, or fuel microbial biogeochemical reactions [*Findlay and Sinsabaugh*, 2003; *Schlautman and Morgan*, 1994]. The presence of NDOM also influences the mobilization and fixation of heavy metals such as As [*Haque et al*., 2007; *Lee et al*., 2005; *Petrovic et al*., 1999] and thus may impact groundwater quality in the course of hydrogeologic projects such as aquifer storage and recovery and aquifer recharge [*Arthur et al*., 2002; *Pavelic et al*., 2005]. The knowledge of NDOM and its behavior in groundwater remains limited, however due to aquifer heterogeneity. Consequently, understanding sources and sinks of NDOM becomes difficult due to factors including variable flow dynamics, multiple coupled biotic-abiotic interactions, and systematic sampling of NDOM from the subsurface.

Among the abiotic interactions in karst aquifers that involve NDOM are sorption and dissolution/precipitation reactions of minerals. The sorption of NDOM onto inorganic solid surfaces may control the chemical behavior of the solids [*Davis*, 1982; *Jin and Zimmerman*, 2010]. Organic solutes have been shown to enhance carbonate mineral dissolution or at least inhibit precipitation [*Inskeep and Bloom*, 1986; *Wu and Grant*, 2002]. At other times, organic matter (OM) sorption has been shown to inhibit carbonate dissolution, possibly due to surface protection, and even enhance carbonate precipitation [*Hoch et al*., 2000; *Jin and Zimmerman*, 2010; *Lin and Singer*, 2005]. Enhanced carbonate dissolution may lead to geological hazards such as land surface subsidence [*Wu*, 2003] and may act as a positive feedback on the development of karst aquifer permeability and reactions with NDOM [*Moore et al*., 2010].

Subsurface microbes produce, consume, and transform NDOM and, in doing so, mediate biogeochemical redox reactions that alter inorganic species in an aquifer such as calcium and oxygen [*Chapelle et al*., 2002; *Lovley and Chapelle*, 1995]. One simplifying assumption in the study of subsurface microbial metabolism is the almost complete reliance on NDOM supplied from the surface [*Hancock et al*., 2005]. Concentrations of dissolved organic carbon (DOC) and terminal electron acceptors such as O_2 and NO_3^- should decrease along groundwater flow paths from recharge areas due to microbial decomposition of NDOM, while the products of NDOM mineralization, such as dissolved inorganic carbon (DIC), should display simultaneous increases in concentrations. Strong attenuation of DOC concentrations along groundwater flow paths has been observed in many previous studies [*Alberic and Lepiller*, 1998; *Aravena et al*., 2004; *Lindroos et al*., 2002; *McCarthy et al*., 1996; *Pabich et al*., 2001; *Rauch and Drewes*, 2004]. Changes in DOC concentrations along flow paths in karst systems may be employed to identify sources and movement of groundwater [*Batiot et al*., 2003; *Lee and Krothe*, 2001]. However, the changes in DOC concentrations can also result from mixing of multiple sources, mineral dissolution/precipitation, and other abiotic reactions. Because of the number of processes that may change DOC concentrations, a multiple tracer approach combining the DOC, DIC, and dissolved ion concentrations, as well as stable isotopes and OM composition, may be useful in discriminating among the various possible processes.

This study uses such a multiple tracer approach to examine the relative magnitudes of source-water mixing and abiotic and biotic processes that control the quantity and quality of organic and inorganic C over a period of about 6 years in the O'Leno Sink-Rise portion of the Santa Fe River in north Florida. The Sink-Rise system is an ideal location for this type of study for a number of reasons, including lithologic variations, variations in the DOC concentrations of water, seasonality, and much preliminary data. Lithologically, the Miocene Hawthorn Group, which acts as a leaky aquitard in the Santa Fe River watersheds, is present in only half of the basin, thereby separates the UFA into confined and unconfined portions. This separation allows the collection of water from the aquifer with varying degrees of mixing between NDOM-rich surface waters and NDOM-poor groundwater. The large seasonality in precipitation and associated NDOM flux to the aquifer allows for a clear separation between processes occurring during high and low river flow periods. Lastly, a number of previous hydrological and hydrogeological studies carried out at this site [*Langston et al*., 2012; *Martin and Dean*, 2001; *Moore et al*., 2009, 2010; *Ritorto et al*., 2009; *Screaton et al*.,

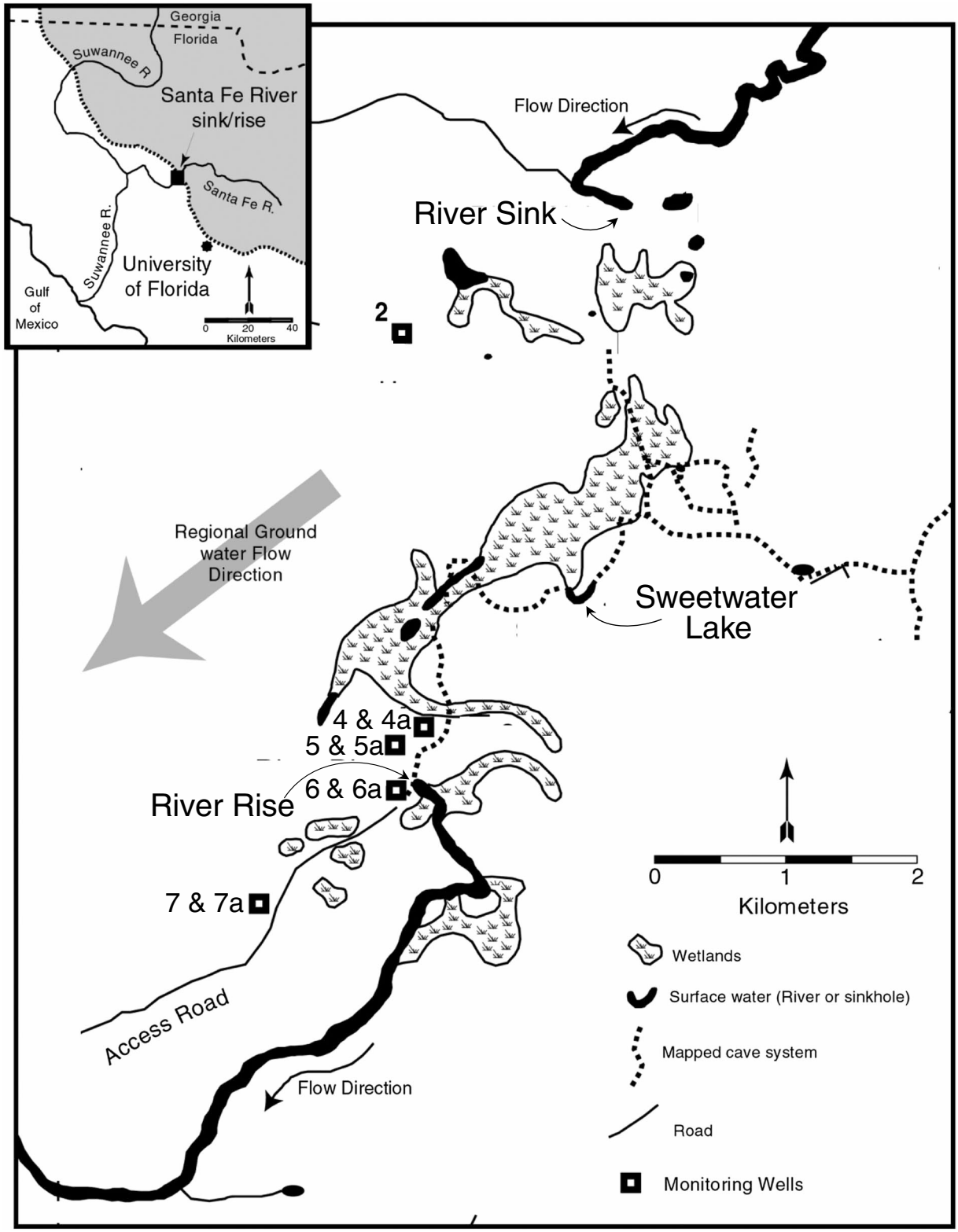

Figure 1. Study area showing surface water sampling locations (Santa Fe River Sink, River Rise, and Sweetwater Lake), deep groundwater monitoring wells (2, 4, 5, 6, and 7), and paired shallow water wells (4a, 5a, 6a, and 7a). Inset shows regional setting; shaded where the upper Floridan aquifer is confined by the Hawthorn Group, unconfined to the southwest.

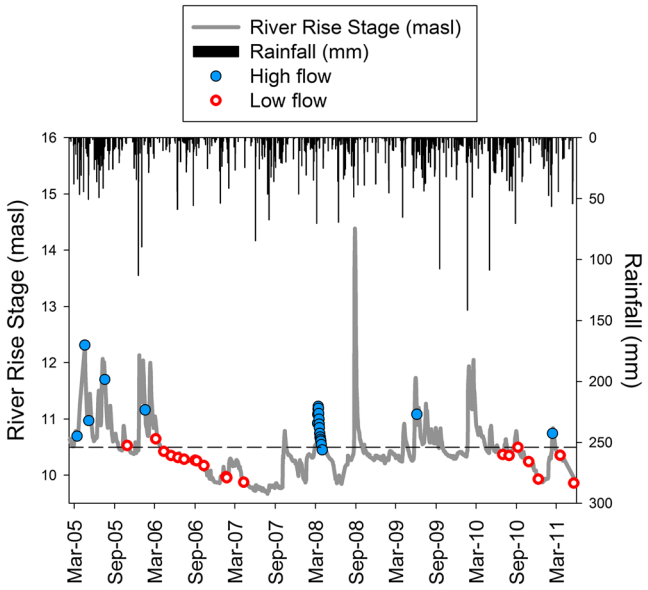

Figure 2. Stage of the Santa Fe River at the River Rise (in meters above sea level), rainfall within O'Leno State Park, and sampling episodes designated as low flow (open circles) or high flow (closed circles). The dashed line indicates the average River Rise stage of 10.5 masl during the 6 year sampling period.

2004] provide the necessary framework upon which to examine the biotic and abiotic NDOM transformation processes, which occur in the complex system of karst aquifers.

2. Study Area

The Santa Fe River in north Florida (Figure 1) flows west from Lake Santa Fe and surrounding wetlands for about 40 km until it reaches the Cody Scarp, which represents the edge of the clay-dominated Hawthorn Group and thus the separation of confined and unconfined UFA. At this location, the river sinks into a 36 m deep sinkhole at the Santa Fe River Sink in O'Leno State Park. The river flows ~7 km underground, over a period of 13 h to 7 days, through a network of conduits in the karstic UFA until it reemerges at the Santa Fe River Rise, a first-magnitude spring, marking the start of the lower Santa Fe River which flows to the Suwannee River [*Martin and Dean*, 2001; *Moore et al*., 2009]. The Sweetwater Lake is a karst window that occurs between the Sink and the Rise. The lake is connected to the Rise by a single conduit, but its connection with the Sink has not been fully mapped. In this region, the UFA extends from the upper Eocene Ocala Limestone to the lower confining unit of the lower Eocene Cedar Key Formation (mainly limestone) [*Miller*, 1986]. The UFA is about 430 m thick but unconfined at the surface as here it is only covered by a thin veneer of unconsolidated sediments [*Miller*, 1986]. Porosity and matrix permeability within the Sink-Rise system have been reported as ~30% and 10^{-13} m^2, respectively [*Budd and Vacher*, 2004; *Florea and Vacher*, 2006].

Previous work has shown that the water discharging at the Rise ranges in chemistry, from similar to water flowing into the Sink to similar to groundwater sampled from nearby monitoring wells [*Martin and Dean*, 2001; *Moore et al*., 2009; *Screaton et al*., 2004]. This work indicates that at high flow, discharge at the Rise mostly derives from water entering the conduit system at the Sink, while during low flow, discharge at the Rise largely comes from groundwater draining from the surrounding aquifer matrix into the conduit system, i.e., diffuse recharge [*Martin and Dean*, 2001]. In addition to these two water sources, water was found to upwell from >400 m depth in the aquifer [*Moore et al*., 2009]. The fractions contributed by each of these three sources depend on variations in head gradients between the conduit and surrounding aquifer matrix, which are influenced by precipitation, evapotranspiration, and river stage [*Moore et al*., 2009].

3. Methods

3.1. Field Sampling

Surface water and groundwater were sampled 44 times between March 2005 and May 2011 quarterly during the first 2 years and thereafter to capture hydrologic variability of the river as it occurred (Figure 2). In addition, sampling took place 7 times over a 3 week period during a storm event of March 2008. The storm event data and interpretation are presented in detail elsewhere [*Jin*, 2012], and only average values from this event are used here. Surface water samples were collected at three sites (the Sink, the Rise, and the Sweetwater Lake) in O'Leno State Park (Figure 1). Groundwater samples were collected from nine groundwater monitoring wells, including four nested wells, where the deep wells (W4, 5, 6, and 7) were screened at the approximate depth of the conduits ~30 m below the ground surface, and where the shallow

well (W4a, 5a, 6a, and 7a) were screened at the water table ~10 m below the ground surface. Detailed information about the location of wells can be found in Table S1 in the supporting information.

Surface water samples were collected from the shore using a peristaltic pump (Geotech Geopump 2) attached to tubing lowered to ~1 m below the surface within a spring boil at the River Rise and the Sweetwater Lake or at the deepest part of the River Sink. Groundwater samples were collected using a Grundfos II submersible pump attached to tubing and lowered to a depth of approximately 1 m below the water level in the well. Prior to sampling each well, water level was measured and recorded; no drawdown was observed during pumping. Before recording values of field parameters or collecting samples, tubing was flushed with at least 2 L of ambient surface water, which represented in excess of 4 times the tubing volume for surface water sampling, or with at least three well volumes for groundwater. Following flushing, field parameters including specific conductivity (SpC), pH, dissolved oxygen (DO), and water temperature were measured with an YSI multiprobe (model 556) placed in a free-flow cell.

Samples for inorganic carbon concentrations and C stable isotope analyses were collected unfiltered, in glass vials leaving no airspace, and immediately preserved with $HgCl_2$. Previous tests showed that sample filtration did not change inorganic carbon concentrations in these samples [*Jin*, 2012], and thus, the term "dissolved inorganic carbon" is used henceforth. All other samples were filtered in the field with 0.45 μm pore size Geotech dispos-a-filter™ capsules. Samples for DOC analysis were collected in 40 mL amber glass vials that had been precombusted (450°C, 4 h), and immediately preserved with 1 M HCl to a pH ~3. Samples for anion and alkalinity (Alk) analyses were collected in high-density polyethylene bottles with no preservatives added. Samples for cation analyses were collected in 20 mL acid-washed bottles and preserved with trace metal grade nitric acid to a pH <2. All the samples were stored on ice and in the dark while in the field and refrigerated in the laboratory until analyzed.

3.2. Chemical Analyses

The DOC concentrations of the acidified samples were measured on a Shimadzu TOC-5000A via high-temperature catalyzed combustion and measurement of CO_2 by IR detection, after sparging for 2 min with C-free air to remove inorganic C. For samples collected in 2007 and 2008, the DIC concentration was measured on unacidified samples using the same total organic carbon analyzer. For both DOC and DIC, three to five injections of a 60 μL sample were measured. Only data with $<5\%$ coefficient of variance were accepted (internal standards, $>98\%$ of samples passed this criteria, and analytical precision ±0.2 mg/L). For samples collected before 2007 and after 2008, the DIC concentrations were measured on an automated coulometer. The DIC results were standardized using a $KHCO_3$ solution of known concentration, and the accuracy was calculated to be ±0.1 mg/L. Stable isotopes of the DIC ($\delta^{13}C_{DIC}$) were measured using a ThermoFinnigan MAT 252 mass spectrometer. The isotopic results are expressed in standard delta notation relative to Vienna Peedee belemnite. The analytical precision based on replication of standards was ±0.1‰.

For samples collected from March 2005 to April 2007, concentrations of major ions (Na^+, K^+, Ca^{2+}, Mg^{2+}, F^-, Cl^-, and SO_4^{2-}, with a precision of $<3\%$) and alkalinity were determined by a National Environmental Laboratory Accreditation Conference-certified laboratory (Advanced Environment Laboratories, Inc., Gainesville, FL) in accordance with a protocol developed by the U.S. Environment Protection Agency [*U.S. Environment Protection Agency*, 1983]. These results have been reported previously [*Martin and Moore*, 2007; *Moore et al.*, 2009]. For samples collected after April 2007, the concentrations of major ions were measured on an automated Dionex DX500 ion chromatograph in the Department of Geological Sciences at University of Florida. Those samples were titrated and measured for alkalinity at room temperature, within 24 h of sample collection. The relative standard deviation of internal standards measured along with the samples had a precision of $<3\%$, and charge balance errors were $<5\%$ in 221 out of 248 samples. For the DOC, DIC, stable isotope, and major ions analyses, all the blanks and replicates were treated in the same manner as the samples. Saturation indices with respect to calcite and dolomite ($SI_{calcite}$ and $SI_{dolomite}$) were calculated using the geochemical code, PHREEQCI, version 2.18.3-5570. The SI for a given mineral is calculated as

$$SI = \log\left(\frac{IAP}{K}\right) \quad (1)$$

where IAP is the ion activity product and K is the equilibrium constant. Thermodynamic data were provided

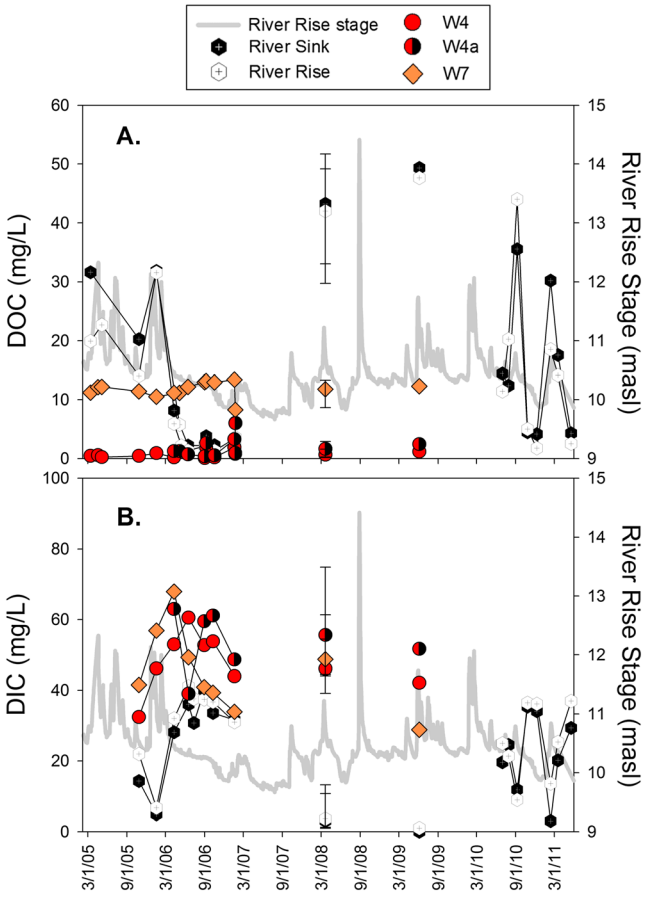

Figure 3. Time series data of (a) DOC and (b) DIC concentration during the 6 year study period. Shown are two representative surface water sites (River Sink and River Rise, hexagon symbols) and three representative wells sites (W4, W4a, and W7). Error bars represent the ranges of DOC and DIC concentrations of the samples collected during the March 2008 storm event. Stage at the River Rise is shown as a thick gray line.

by the phreeqc.dat database. The partial pressure of CO_2 (P_{CO2}) for each sample collected was calculated using the same geochemical code and database.

3.3. Hydrologic Data

Rainfall and river stage data were obtained from Suwannee River Water Management District data website (SRWMD, http://www.srwmd.state.fl.us/documentcenterii.aspx). The daily precipitation in O'Leno State Park is represented by the data from SRWMD rain station #240 (29°55'12'N, 82°36'27'W) collected by an automated rain gauge. Detailed information on the monitoring of stage of the Santa Fe River at the River Rise using an automatic Van Essen CTD Diver pressure transducer has been described earlier [*Martin and Moore*, 2007; *Moore et al.*, 2009; *Screaton et al.*, 2004].

4. Results

4.1. Hydrologic Conditions

During the 6 year study period, the Rise stage ranged from 9.7 to 14.4 masl (meters above sea level; 10.5 ± 0.5 = mean ± standard deviation used throughout text, median stage = 10.4 masl) and generally followed variations in precipitation (Figure 2). The average river stage of the Santa Fe River at O'Leno State Park (measured at U.S. Geological Survey gauging station #02321898, 29°54'51"N, 82°34'48"W from 12 March 1980 to 30 November 2011) is 10.6 masl, suggesting that the 6 year sampling period examined represents longer-term hydrologic conditions of the study area. A lag of 1 to 3 days was observed between rain event and rise in river stage. Although the wet period in north Florida is usually from June through September, rainfall did not strictly follow this pattern. During the study period, 2005 and early 2006 were particularly wet (average Rise stage = 10.9 masl, average rainfall = 3.7 mm/d) and summer 2006 through 2008 were almost drought-like conditions (average Rise stage = 10.2 masl, average rainfall = 2.9 mm/d). The 44 sampling campaigns were divided into "low-flow" (20) and "high-flow" (24) conditions (Figure 2). Periods with a River Rise stage greater than 10.6 masl, the 30 year mean river stage of the Santa Fe River at O'Leno State Park, were defined as high-flow conditions, while those with stage lower than 10.6 masl were defined as low-flow conditions. The River Rise stage ranged from 9.9 to 10.6 masl (10.2 ± 0.2 masl) during low flow and from 10.7 to 12.3 masl (11.0 ± 0.4 masl) during high-flow conditions. For statistical purposes, the high-resolution samplings of the March 2008 storm event are treated as a single-high-flow data point of 21 March 2008.

4.2. Organic Carbon Concentration Variations

Surface water DOC concentrations ranged from 1.3 to 51.7 mg/L (31.4 ± 16.4 mg/L, $n = 89$) and were significantly ($p < 0.001$) greater and more temporally variable than those of the groundwater samples, which ranged from 0.1 to 5.9 mg/L (1.7 ± 1.1 mg/L, $n = 94$, excluding W7 and W7a) (Figure 3a). The elevated DOC concentrations in surface water occurred during high flow, ranging from 18.5 to 49.3 mg/L (34.0 ± 11.4 mg/L, $n = 14$) and were significantly ($p < 0.001$) lower during low flow, ranging from 1.3 to 44.0 mg/L (10.3 ± 10.5 mg/L, $n = 27$). In

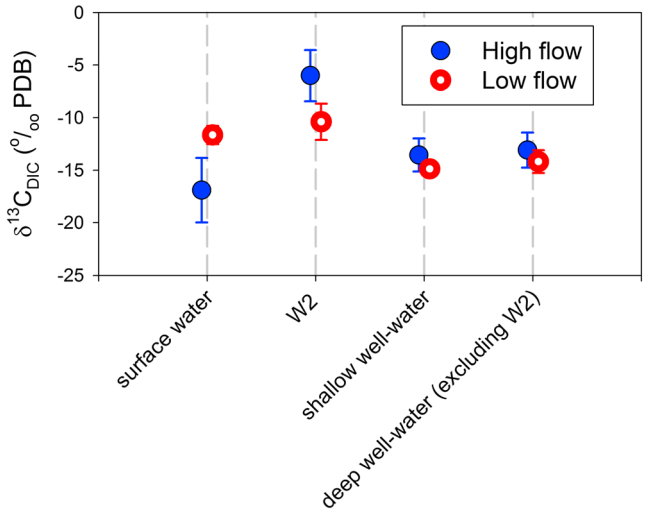

Figure 4. Average stable carbon isotope signatures of surface water and deep and shallow well water sites during high-flow and low-flow periods. Error bars represent the standard deviation of $\delta^{13}C_{DIC}$ measured in each sample grouping.

contrast, the groundwater DOC concentrations were always lower than surface water, except for W7 and W7a, and were not significantly different ($p = 0.34$) during high flow (2.0 ± 1.3 mg/L, $n = 28$) and low flow (1.7 ± 1.1 mg/L, $n = 24$).

The DOC concentrations of the nested wells, though different, appeared to vary in concert (Figure S1 in the supporting information). Two nested well pairs (W4 and W4a and W6 and W6a) displayed greater DOC concentrations in the shallow wells versus deep wells. For example, the DOC concentration in W4a (shallow) ranged from 0.3 to 3.3 mg/L (1.7 ± 1.1 mg/L, $n = 11$) while that in W4 ranged from 0.1 to 1.9 mg/L (0.7 ± 0.5 mg/L, $n = 16$). In contrast, the DOC concentrations in deep well W5 ranged from 1.2 to 5.9 mg/L, (2.1 ± 1.2 mg/L, $n = 16$), which were greater than shallow well W5a, where they ranged from 0.8 to 2.4 mg/L (1.4 ± 0.5 mg/L, $n = 11$). The concentrations of DOC at W7 and W7a ranged from 8.3 to 13.4 mg/L (11.9 ± 1.2 mg/L, $n = 16$) and 3.1 to 7.8 mg/L (5.9 ± 1.7 mg/L, $n = 11$), respectively. Groundwater at W7 and W7a had significantly higher DOC concentrations than other sites ($p < 0.001$) and higher DOC concentrations in deep versus shallow well water than the other nested wells. During the March 2008 high-resolution sampling, the DOC concentrations were constantly low in groundwater (excluding W7 and W7a), while they remained high in surface water (Figure S1 in the supporting information).

4.3. Inorganic Carbon Concentration Variations

The surface water DIC ranged from 0.0 to 37.6 mg/L (11.9 ± 12.8 mg/L, $n = 83$) and was significantly lower and less variable than the DIC in groundwater ($p < 0.001$), which ranged from 21.0 to 96.5 mg/L (48.2 ± 12.7 mg/L, $n = 117$) (Figure 3b). The surface water DIC concentrations were significantly lower during high flow (4.5 ± 3.9 mg/L, $n = 10$) than during low-flow (28.2 ± 8.1 mg/L, $n = 28$) conditions ($p < 0.001$). The groundwater DIC levels were also significantly lower during high flow (42.5 ± 10.2 mg/L, $n = 23$) than during low flow (51.2 ± 11.8 mg/L, $n = 40$) ($p < 0.01$).

Similar to the DOC patterns, the DIC concentrations were generally higher in shallow well samples, which ranged from 31.0 to 96.5 mg/L (53.8 ± 14.4 mg/L, $n = 48$), than their paired deep wells, which ranged from 21.0 to 67.9 mg/L (44.3 ± 9.6 mg/L, $n = 69$). For example, the DIC concentration in W4a ranged from 44.5 to 74.8 mg/L (56.3 ± 8.4 mg/L, $n = 12$) while that of W4 ranged from 32.5 to 61.3 mg/L (46.3 ± 7.5 mg/L, $n = 14$), and the average DIC concentration in W5a (71.5 ± 9.8 mg/L, $n = 12$) was much greater than that in W5 (34.1 ± 8.5 mg/L, $n = 14$). In contrast, W7 had higher DIC (46.6 ± 9.7 mg/L, $n = 14$) than W7a (40.5 ± 8.2 mg/L, $n = 12$). During the March 2008 high-resolution sampling, the DIC concentrations were high in groundwater and low in surface water (Figure S1 in the supporting information).

4.4. Stable Carbon Isotopic Variations

Overall, surface water $\delta^{13}C_{DIC}$, ranging from −22.8‰ to −10.2‰ (−14.4 ± 3.5‰, $n = 45$), was not significantly different from that of groundwater samples excluding those from W2, which ranged from −15.6‰ to −9.3‰ (−13.6 ± 1.6‰, $n = 50$) (Figure 4). However, surface water $\delta^{13}C_{DIC}$ was significantly ($p < 0.001$) heavier during low-flow (−11.6 ± 0.9‰, $n = 21$) compared to high-flow (−16.9 ± 1.9‰, $n = 12$) conditions. In contrast, groundwater remained relatively temporally and spatially constant (high flow: −13.6 ± 2.1‰ versus low flow: −13.8 ± 1.9‰ and shallow wells: −13.8 ± 1.5‰ versus deep wells: −13.3 ± 1.6‰). Groundwater from W2 displayed distinct $\delta^{13}C_{DIC}$ values, which ranged from −11.6‰ to −4.0‰ ($n = 7$).

Table 1. Water Chemistry of Samples Collected in the Santa Fe River Sink-Rise System[a]

Parameter	Surface Water		Shallow Well Water		Deep Well Water (Excluding W2)		Well W2	
	High Flow	Low Flow	High Flow	Low Flow	High Flow	Low Flow	High Flow	Low Flow
DIC (mg/L)	4.5 ± 3.9 (10)	28.2 ± 8.1 (28)	46.2 ± 11.7 (8)	57.6 ± 12.0 (16)	39.4 ± 9.6 (12)	45.7 ± 10.2 (20)	45.0 ± 6.4 (3)	52.6 ± 2.1 (4)
DOC (mg/L)	34.0 ± 11.4 (14)	10.3 ± 10.5 (27)	3.7 ± 2.0 (8)	2.5 ± 1.3 (12)	4.2 ± 4.6 (24)	4.2 ± 4.9 (16)	2.1 ± 0.7 (4)	1.3 ± 0.2 (3)
$\delta^{13}C_{DIC}$ (‰)	−16.9 ± 1.9 (12)	−11.6 ± 0.9(21)	−14.1 ± 1.4 (4)	−14.9 ± 0.5 (5)	−14.4 ± 0.7 (4)	−14.2 ± 1.1(5)	−8.7 ± 0.9 (3)	−10.4 ± 1.7 (3)
Cl^- (mg/L)	14.7 ± 2.4 (20)	14.1 ± 3.1 (32)	11.5 ± 3.4 (4)	9.4 ± 2.4 (16)	9.2 ± 4.6 (40)	9.0 ± 3.8 (24)	50.4 ± 10.7 (4)	45.7 ± 17.1 (6)
SO_4^{2-} (mg/L)	21.8 ± 12.4 (17)	62.2 ± 32.8 (32)	18.9 ± 7.9 (4)	21.4 ± 13.4 (16)	9.7 ± 6.8 (23)	6.0 ± 6.3 (18)	369.8 ± 94.8 (4)	386.3 ± 75.5 (6)
Ca^{2+} (mg/L)	29.8 ± 31.3 (20)	56.6 ± 18.0 (32)	139.2 ± 256.3 (4)	101.2 ± 14.0 (16)	81.4 ± 25.6 (40)	81.5 ± 11.0 (24)	207.6 ± 116.9 (4)	174.8 ± 20.5 (6)
Na^+ (mg/L)	6.6 ± 1.7 (20)	8.3 ± 1.9 (32)	7.1 ± 1.1 (4)	5.4 ± 1.2 (16)	4.4 ± 2.0 (40)	4.0 ± 1.3 (24)	29.2 ± 4.3 (4)	33.8 ± 5.3 (6)
Mg^{2+} (mg/L)	4.4 ± 2.5 (20)	12.4 ± 4.1 (32)	10.5 ± 5.6 (4)	1.7 ± 0.2 (16)	2.6 ± 2.7 (40)	1.8 ± 1.3 (24)	30.2 ± 6.2 (4)	44.4 ± 9.9 (6)
K^+ (mg/L)	1.1 ± 0.5 (20)	0.9 ± 0.3 (32)	1.9 ± 1.9 (4)	1.7 ± 2.9 (16)	0.5 ± 0.2 (39)	0.5 ± 0.2 (24)	2.4 ± 0.3 (4)	2.8 ± 0.6 (6)
Alkalinity (mg/L $CaCO_3$)	45.0 ± 31.1 (20)	174.8 ± 67.9 (32)	510.7 ± 111.1 (4)	226.8 ± 36.1 (16)	232.1 ± 81.7 (40)	191.8 ± 27.5 (24)	263.5 ± 136.4 (4)	207.0 ± 5.1 (6)
pH	6.7 ± 0.4 (19)	7.3 ± 0.5 (30)	7.2 ± 0.1 (4)	6.9 ± 0.2 (16)	6.8 ± 0.2 (40)	6.9 ± 0.2 (24)	6.8 ± 0.3 (4)	6.8 ± 0.2 (6)
SpC (µs/cm)	166.4 ± 75.1 (19)	408.0 ± 113.2 (32)	439.0 ± 88.0 (4)	488.3 ± 55.1 (16)	438.4 ± 52.2 (40)	406.8 ± 48.7 (24)	1082.0 ± 120.2 (4)	1165.7 ± 155.9 (6)
DO (mg/L)	4.8 ± 1.8 (19)	2.8 ± 2.1 (32)	2.7 ± 2.3 (4)	1.3 ± 1.3 (16)	0.5 ± 0.5 (40)	0.5 ± 0.6 (24)	0.2 ± 0.1 (4)	0.3 ± 0.1 (6)
Temperature (°C)	19.3 ± 4.3 (19)	22.5 ± 3.4 (32)	20.7 ± 0.7 (4)	20.8 ± 0.4 (16)	21.0 ± 0.3 (40)	21.1 ± 0.3 (24)	25.2 ± 1.1 (4)	25.5 ± 0.6 (6)

[a]Data are mean ± standard deviation (number of samples) grouped by location and flow condition.

4.5. Variations in Major Ion Concentrations and Other Water Chemistry Parameters

Information about major ion concentrations and other water chemistry parameters of water samples from the Sink-Rise system are presented in Table 1. Shallow well water often showed greater ion concentrations and SpC, yet comparable water temperature, than deep well water (excluding W2). Water at W2 displayed the highest ion concentrations, SpC, and water temperature among all the surface water and well water samples collected. When river flow conditions changed from high to low flow, the concentrations of SO_4^{2-}, Ca^{2+}, Mg^{2+}, and Alk and SpC of surface water doubled or tripled, while concentrations of Cl^-, Na^+, and K^+ remained relatively unchanged. The changes in water chemistry in shallow and deep well water during the transition between flow conditions were generally smaller than those of surface water. Surface water possessed the highest DO concentrations among all samples collected, followed by shallow well water, while the deep well water displayed the lowest DO. When river flow shifted from high to low, the concentrations of DO decreased in surface and shallow well water, but did not change in deep well water. The pH was close to neutral in both surface and groundwater, with surface water showing greater variation than groundwater.

5. Discussion

The chemical data presented above were generally, bimodally distributed; thus, we assume that they reflect two end-member water types (and C sources): a DOC-rich/DIC-poor/$\delta^{13}C_{DIC}$-depleted surface water component (herein referred to as the DOC-rich source) and a DOC-poor/DIC-rich/$\delta^{13}C_{DIC}$-enriched groundwater component (DIC-rich source). Given that the DOC-rich source predominated in surface water during high flow and that the DIC arising from the mineralization of plant-derived OM is expected to be relatively depleted in ^{13}C [*Clark and Fritz*, 1997], the DOC-rich source appears to have originated from wetlands or soil water (*Moore et al.*'s [2009] "allogenic recharge" during high-flow periods). Given that the DIC-rich source was most common in well water samples and had a relatively enriched C isotopic signature closer to that of marine limestone (~0‰) [*Clark and Fritz*, 1997; *Randazzo and Jones*, 1997], the DIC-rich source likely arose from the UFA (*Moore et al.*'s [2009] "diffuse recharge"). These two sources mix where DOC-rich water recharges the aquifer during flow into sinkholes and springs discharge

DIC-rich water to the river. Water from W2 exhibited similar DOC and DIC concentrations as water from other wells, while showing a distinct $\delta^{13}C_{DIC}$ signature and significantly higher ion concentrations, SpC, and water temperature than groundwater elsewhere. These observations indicated that a third water source, probably water upwelling from deep within the aquifer (*Moore et al.*'s [2009] "deepwater recharge"), may exist and have more influences on W2 than the other well sites.

In the following discussion, the DOC-rich, DIC-rich, and deepwater sources are referred to as soil water, groundwater, and deepwater end-members, respectively. Variable mixing of these three end-members appears to control some of the spatiotemporal variations in organic and inorganic C concentrations in the Sink-Rise system, but additional changes could result from biogeochemical reactions. Consequently, in the following, we develop a model to quantify the fraction of each end-member water source in each sample and subsequently to assess biogeochemical reactions that control distributions of organic and inorganic C in the Sink-Rise system.

5.1. Source Water Mixing Model

In a previous study on the O'Leno Sink-Rise system, *Moore et al*. [2009] used the distributions of Mg^{2+} and SO_4^{2-} concentrations to quantify the fraction of three end-member water sources (i.e., allogenic recharge, diffuse recharge, and deepwater recharge) in each sample. The mixing model used in the following was modified from the one presented by *Moore et al*. [2009]. Unlike *Moore et al*. [2009], the concentrations of Mg were not used here due to the fact that Mg^{2+} may be involved in carbonate reactions [*de Montety et al*., 2011]. Instead, the concentrations of Na^+ and Cl^- were used to define the mixing model, assuming these elements are conservative in this system [*Martin and Dean*, 2001]. Na^+ and Cl^- showed a better linear correlation ($R^2 = 0.80$, $p < 0.0001$; Figure S2 in the supporting information) than Mg^{2+} and SO_4^{2-}. In addition, the average molar Na/Cl ratio in the Sink-Rise system is 0.87 ± 0.32 ($n = 248$), similar to that of seawater (0.86), suggesting that the primary source of these ions is sea spray [*Grubbs*, 1998]. Similar to the study of *Moore et al*. [2009], SO_4^{2-} was still included to estimate the contribution of the sulfate-rich deepwater end-member that flows upward at ~1 m/yr. Sulfate reduction was unlikely to have occurred in the system since DO was present in all samples. In fact, sulfate concentrations were highest in the deep aquifer where DO was the lowest, suggesting that SO_4^{2-} behaved conservatively in this system.

The concentrations of Na^+, Cl^-, and SO_4^{2-} in three specific samples were used to define the ion compositions of the three end-member water sources (given in Table S2 in the supporting information). The groundwater end-member was best represented by deep well water collected at W4, which contained low DOC and salt concentrations, elevated DIC concentrations (Figure 3 and Figure S2 in the supporting information), and heavy $\delta^{13}C_{DIC}$ signatures. Water from W4 also had a smaller coefficient of variation in concentrations of Na^+ (0.0.06), Cl^- (0.06), and SO_4^{2-} (0.1) compared to water from other wells, indicating its isolation from diffuse surface water intrusion and thus its chemistry reflecting equilibration with Floridan aquifer rocks [e.g., *Moore et al*., 2009]. Ion concentration data from W4 collected on 17 January 2007 was used as the groundwater end-member because it was collected during one of the lowest-flow periods and had among the lowest concentrations in Na^+ and Cl^- of the 22 samples collected from W4, indicating that it may have undergone the least dilution by other water sources.

The soil water end-member was best represented by ion concentrations in River Sink samples collected during high-flow conditions, reflecting rainwater that evolved as surface flow. Ion concentrations in the Sink water were fairly uniform during high-flow conditions, with Na^+, Cl^-, and SO_4^{2-} concentrations of 8.0 ± 1.4, 14.7 ± 2.0, and 10.4 ± 1.8 mg/L, respectively ($n = 20$). The sample collected from the Sink on 28 March 2008 was selected to represent the composition of the soil water end-member for the model as it possessed the highest concentrations of both Na^+ and Cl^- among all the 34 samples collected from the Sink.

This deep aquifer end-member is similar to the groundwater end-member in having low DOC and high DIC concentrations (Figure 3 and Figure S2 in the supporting information), but differs in its elevated SO_4^{2-}, Ca^{2+}, and Mg^{2+} concentrations [*Moore et al*., 2009, 2010] (Figure 4). The deepwater end-member is best represented by water samples at W2, located ~2 km southwest of the River Sink. It was chosen as the end-member in that ion chemistry varied little over time (coefficients of variation of 0.15, 0.22 and 0.18 for Na^+, Cl^-, and SO_4^{2-}, respectively) and had the highest ion concentrations, particularly during the extreme low flow of 1 January 2007 which was chosen as the sample chemistry for the model (Table S2 in the supporting information).

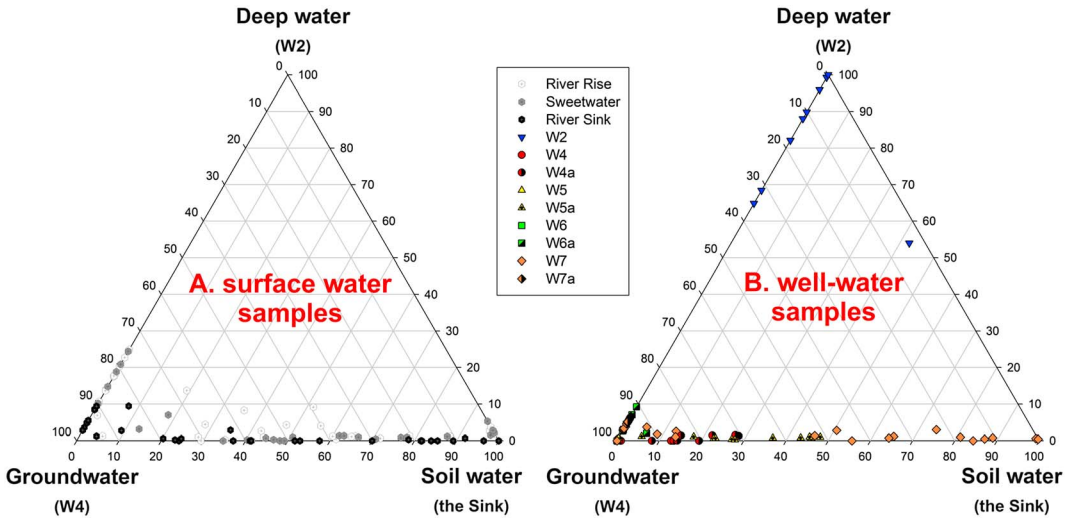

Figure 5. Results of the water source mixing model shown as the fraction (in %) of soil water, groundwater, and deepwater theoretical endmembers in each (a) surface water sample and (b) well water sample collected in the Sink-Rise system over the 6 year study period.

The mixing model is based on mass balance calculations assuming the following relationships:

$$f_{soil} + f_{gw} + f_{deep} = 1 \quad (2)$$

$$SO4_n = f_{soil}SO4_{soil} + f_{gw}SO4_{gw} + f_{deep}SO4_{deep} \quad (3)$$

$$Na_n = f_{soil}Na_{soil} + f_{gw}Na_{gw} + f_{deep}Na_{deep} \quad (4)$$

$$Cl_n = f_{soil}Cl_{soil} + f_{gw}Cl_{gw} + f_{deep}Cl_{deep} \quad (5)$$

where f is the volumetric fractions of each end-member: "soil," "gw," and "deep" represent soil water, groundwater, and deepwater respectively. $SO4_n$, Na_n, and Cl_n are the concentrations of SO_4^{2-}, Na^+, and Cl^- in any given water sample n. These equations were solved iteratively and simultaneously using Microsoft Excel's Solver Add-in to yield the fraction of each end-member in each sample, while minimizing the residuals of equations (3) to (5).

5.2. Source Water Mixing Patterns

The results of this mixing model for all water samples are shown in Figure 5 (also see Table S3 in the supporting information). Surface waters (i.e., the River Sink, River Rise, and Sweetwater) contained all three end-members. The deep source typically made up <10% of the sample. Surface water contained a greater fraction of soil water end-member during high flow (60 ± 25%) than low flow (2 ± 7%) and more of the groundwater end-member during low (38 ± 25%) than high flow (87 ± 8%). In contrast, the samples collected from wells are largely composed of the groundwater end-member, whether in shallow or deep wells. On average, approximately 86% and 89% of the well water was derived from the groundwater end-member and approximately 13% and 10% could be attributed to the soil water end-member during high flow and low flow, respectively. Water collected from W4a, W5a, and W7 displayed higher contributions from the soil water end-member (15.7%, 31.0%, and 47.0% on average, respectively) than water from other wells, regardless of the flow conditions. The deepwater end-member usually made only limited contributions to both surface water (1 ± 2% during high and 11 ± 7% during low flow) and well water (1 ± 2% during high and 1 ± 3% during low flow) and unsurprisingly represented the greatest source of water at site W2 (92 ± 14% during high flow and 88 ± 17% during low flow).

Some of the simplifying assumptions of this model are that (1) there are exactly three chemically distinct sources of water in the system; (2) Na^+, Cl^-, and SO_4^{2-} concentrations behave conservatively in the system; that is, they do not vary temporally or spatially but only vary in concentration due to mixing of the water sources; and (3) ion concentrations used in the model do, in fact, represent the composition of the three water sources. In order to evaluate the effects of small violations of the assumptions of the mixing model, a

series of sensitivity analyses were performed in which mixing proportions were recalculated after adding or subtracting a standard deviation of the variance in each ion concentration defining each end-member (Na^+, Cl^-, and SO_4^{2-}). These tests resulted in changes in the volumetric mixing fraction of each end-member of up to 17%. One possible illustration of model error is the unlikely finding that the deepwater end-member represented 8–9% of River Sink water and 20–24% of Sweetwater Lake water during a low-flow period. While it is possible that deep water mixes into the river upstream of the sink (there are springs above the sink), this result is more likely due to model error, i.e., violation of the assumptions of the model. On the other hand, the always increasing proportions of deepwater fraction from the Sink to the Sweetwater Lake to the Rise are just as one would expect. Regardless, the average change in the contribution of any water source was 4.8%, 5.0%, and 3.4% for a 1 standard deviation change in the Na^+, Cl^-, and SO_4^{2-} concentration defining any end-member, respectively. And this variability affected each end-member source equally. Thus, while the mixing model was, in a few cases, quite sensitive to the ion concentrations defining each end-member, there was no apparent directional bias in the model results due to the observed natural variability in these concentrations.

5.3. Carbon Dynamics Processes

Three paired biogeochemical processes are most likely to affect C dynamics in this system: (1) microbial mineralization/autotrophic production of NDOM, (2) dissolution/precipitation of carbonate minerals, and (3) NDOM-mineral sorption/desorption. Mineralization and production of NDOM can be generalized by the following reaction:

$$\mathrm{NDOM} + \mathrm{Oxidant} \longleftrightarrow \mathrm{DIC} + \mathrm{H^+} + \mathrm{H_2O} \tag{6}$$

This reaction proceeds to the right for mineralization and to the left for production, assuming eventual transformation of algal biomass to NDOM via processes such as exudation and lysis. During mineralization, NDOM is decomposed to DIC by heterotrophic microbes or during nighttime respiration of subaquatic plants [e.g., *de Montety et al*., 2011] using an oxidant such as free oxygen and releasing protons in the process. Mineralization of NDOM will add isotopically light biogenic C to the water, shifting $\delta^{13}C_{DIC}$ toward values ranging from −15 to −25‰, depending on the photosynthetic pathways (C3 or C4) for organic C production [*Clark and Fritz*, 1997]. The reverse reaction of NDOM mineralization, autotrophy, or the production of OM from inorganic C, increases the concentrations of DOC and oxygen, while decreasing DIC and raising water pH and $\delta^{13}C_{DIC}$ due to preferential uptake of light C [*Drever*, 2002].

Dissolution and precipitation of carbonate minerals (e.g., calcite and dolomite) are common in karst aquatic systems and can be represented by the following equations [*Drever*, 2002]:

$$\mathrm{CaCO_3} + \mathrm{H^+} \longleftrightarrow \mathrm{Ca^{2+}} + \mathrm{HCO_3^-} \tag{7}$$

$$\mathrm{CaMg(CO_3)_2} + 2\mathrm{H^+} \longleftrightarrow \mathrm{Ca^{2+}} + \mathrm{Mg^{2+}} + 2\mathrm{HCO_3^-} \tag{8}$$

Carbonate precipitation was found to account for 88% of the DIC loss in the karstic Ichetucknee Spring Run in north Florida [*de Montety et al*., 2011], although in situ production was not considered as a DIC sink in that study. During carbonate mineral dissolution, the concentrations of Ca^{2+} and Mg^{2+} would increase, as does Alk and SpC of the water. The production of bicarbonate during carbonate dissolution will shift the $\delta^{13}C_{DIC}$ value of the water toward the C isotopic signature of marine limestone (~0‰) [*Clark and Fritz*, 1997; *Randazzo and Jones*, 1997]. The dissolution of these minerals will increase pH, $SI_{calcite}$, and $SI_{dolomite}$ as H^+ is consumed. Lastly, carbonate dissolution may release OM that is incorporated in the structure of the carbonate minerals, as has been observed in a series of desorption experiments using NDOM and Floridan aquifer rocks [*Jin and Zimmerman*, 2010].

Sorption/desorption of NDOM by carbonate minerals could affect both the quantity and the quality of NDOM without altering DIC concentration or $\delta^{13}C_{DIC}$ values [*Findlay and Sinsabaugh*, 2003; *Frimmel*, 1998; *Schwarzenbach et al*., 2003]. Floridan aquifer materials were reported to contain OM in concentrations ranging 0.38 to 1.29 wt % with up to 6.6% of it subject to desorption [*Jin and Zimmerman*, 2010]. The sorption/desorption of NDOM may also influence NDOM composition as higher molecular weight, and thus, more refractory NDOM will be preferentially sorbed by carbonate minerals [*Jin and Zimmerman*, 2010]. The sorption

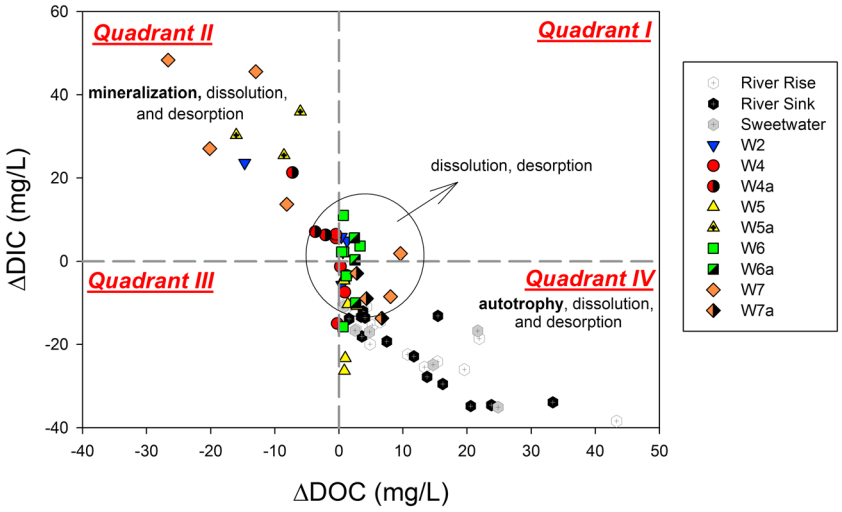

Figure 6. Differences between the model-predicted and measured dissolved inorganic and organic carbon concentrations (ΔDIC and ΔDOC, respectively) in samples from the Sink-Rise system during the 6 year study period. Positive Δ values indicate the production of DOC or DIC, while negative Δ values indicate the consumption of DOC or DIC. Possible biogeochemical processes responsible for shifts are listed in each quadrant. The process judged to be dominant, as discussed in text, is indicated in bold font.

of NDOM has also been shown, in various studies, to either enhance precipitation or inhibit dissolution of carbonate [*Frye and Thomas*, 1993; *Jin and Zimmerman*, 2010; *Thomas et al*., 1993].

5.4. Biogeochemical Influences on Solute Concentrations

Our mixing model results allow the separation of changes in solute concentrations that result from the mixing from those caused by biogeochemical reactions. The effects of biogeochemical reactions on a solute's concentration in a particular sample are calculated as the difference between the model predicted solute concentration and the measured value in the sample. In the following discussion, this difference is reported in Δ notation with a positive value indicating that the reaction provides a source and a negative value indicating that the reaction provides a sink for the dissolved component (Table S4 in the supporting information).

For the C system, the results are shown in a plot of ΔDIC versus ΔDOC values (Figure 6), which is divided into four quadrants to indicate where water gains or loses DIC and/or DOC. Samples may gain DOC (Quadrants I and IV) through autotrophic production or by NDOM released from dissolving aquifer materials. Samples may lose DOC (Quadrants II and III) through mineralization or by sorption of NDOM. Samples may gain DIC (Quadrants I and II) through mineralization of NDOM as well as by carbonate mineral dissolution. Water in this system is unlikely to gain DIC from the atmosphere since surface waters have supersaturated P_{CO2}. The loss of DIC from surface waters (Quadrants III and IV) could occur through either primary production or CO_2 evasion to the atmosphere, but neither of these processes could explain loss of DIC in the subsurface [*Hoffer-French and Herman*, 1989; *Li et al*., 2010]. The DIC could be lost from water anywhere in the system by carbonate precipitation [*de Montety et al*., 2011]. Nearly all water samples plotted within Quadrants II or IV or near the origin in Figure 6. Quadrant IV contains more samples than any other and contains representatives of all hydrologic conditions and all sample locations. A similar approach was taken to illustrate the relationship between biogeochemical ΔDO and ΔDOC (Figure S3 in the supporting information) as well as ΔDIC and ΔCa (Figure S4 in the supporting information) transformations.

The robustness of these results (Δ values) was tested using the model sensitivity analysis described above (section 5.2). Variations in the end-member source water mixing fractions caused by a 1 standard deviation change in the ion concentrations defining each end-member resulted in changes in ΔDIC and ΔDOC values of <4 mg/L and <5 mg/L for surface water samples, respectively, and of <3 mg/L and <0.5 mg/L for groundwater samples, respectively. Thus, were error bars to be added to Figure 6, they would be relatively small compared to the range of calculated chemical effects of biogeochemical processes (Δ values).

5.5. Spatiotemporal Occurrence of Biogeochemical Processes

5.5.1. Autotrophic Production

Samples that show positive ΔDOC and negative ΔDIC values (e.g., Quadrant IV; Figure 6) are likely to reflect autotrophic production, which would consume DIC and produce DOC. Autotrophic production in surface water largely occur via oxygenic photosynthesis, as the production of oxygen (ΔDO = 2.1 ± 2.1 mg/L; Figure S3 in the supporting information) was found in 33 surface water samples collected during the day. Subaquatic vegetation is responsible for most photosynthesis as chlorophyll-a concentrations are low in the clear water below the River Rise [*Heffernan et al*., 2010; *Kurz et al*., 2004]. Our results show that autotrophic production was greater during higher-flow periods evidenced by higher ΔDO and ΔDOC at these times (ΔDO = 3.0 ± 2.4 mg/L and ΔDOC = 20.5 ± 4.1 mg/L) versus lower flow periods (ΔDO = 2.0 ± 2.1 mg/L and ΔDOC = 9.5 ± 10.2 mg/L). This temporal pattern of autotrophy is further supported by the lower ΔDIC and $\delta^{13}C_{DIC}$ values observed during high-flow (−23.7 ± 9.3 mg/L and −18.5 ± 0.3‰) versus low-flow periods (−19.7 ± 8.1 mg/L and −11.8 ± 1.2‰). Enhanced primary production at high flow is unexpected because the elevated NDOM concentrations during high flow should attenuate light penetration and thus limit photosynthesis. Instead, nutrient availability or water temperature may control primary production in the river.

Unlike surface water, most well water samples (particularly those from deep wells) showed no oxygen production (ΔDO = −0.5 ± 0.9 mg/L; Figure S3 in the supporting information), suggesting that autotrophic production in the subsurface is through chemolithoautotrophy. Although chemolithoautotrophy does not appear to vary through time, DOC production varied spatially, with ~6 times greater production occurring near W7 and W7a (ΔDOC = 6.4 ± 1.9 mg/L) than elsewhere. Chemolithoautotrophic production may thus explain the exceptionally high DOC concentrations in water from W7 and W7a (Figure 3). Chemolithoautotrophic microbes have been reported to generate autochthonous OM in air-filled cave and karst systems, some of which support food webs largely based on autochthonous NDOM produced from chemolithoautotrophs [*Birdwell and Engel*, 2009; *Engel et al*., 2004; *Farnleitner et al*., 2005; *Sarbu et al*., 1996; *Vlasceanu et al*., 2000]. For example, *Farnleitner et al*. [2005] presented evidence for the existence of autochthonous microbial communities in the spring water of an alpine karst aquifer. By examining the fluorescent character of NDOM in a karst aquifer in central Texas, *Birdwell and Engel* [2009] concluded that the dominant source of NDOM was in situ chemolithoautotrophic production.

Sulfur, nitrogen, iron, methane, and hydrogen oxidation are among the most common chemolithoautotrophic pathways likely to occur in subsurface systems [*Konhauser*, 2007; *Sarbu et al*., 1996]. While sulfur oxidation may have produced the high sulfate concentrations found in waters near W2 (414.3 ± 77.4 mg/L). However, the neutral pH (6.9 ± 0.2) of this water suggests that dissolution of evaporate minerals such as gypsum or anhydrite was more likely responsible for the high sulfate concentrations at W2, as suggested previously by *Moore et al*. [2009]. Furthermore, N and Fe oxidation can also be ruled out as the main chemolithoautotrophic pathways based on the pH condition of the water. These pathways are unlikely because N oxidation generates nitric acid and Fe oxidation only occurs under pH < 3 [*Konhauser*, 2007], while most deep well water samples collected had neutral pH (7.0 ± 0.3). Although methane oxidation has been previously reported to occur in the UFA [*Opsahl and Chanton*, 2006], this metabolism produces rather than consumes DIC and results in highly depleted C isotopic signatures [*Konhauser*, 2007]. Thus, our data do not suggest methane oxidation in this system. Consequently, the most likely chemolithoautotrophic pathway in the deep aquifer of the Sink-Rise system appears to be hydrogen oxidation. There are both aerobic and anaerobic forms of this metabolism, the best known of which reduces inorganic C to methane. These methanogenic bacteria are known to be ubiquitous in the biosphere's anaerobic habitats, especially when sulfate is not abundant [*Konhauser*, 2007]. Most well water samples plotting in Quadrant IV came from deep wells W4, W5, and W6, where groundwater displayed low sulfate concentrations (<5 mg/L). This coincidence with low sulfate concentrations suggests that the deeper portions of the aquifer in this system may contain active methanogens.

5.5.2. Mineralization of NDOM

Mineralization of NDOM is likely to have occurred in those samples that display negative ΔDOC and ΔDO, and positive ΔDIC values (e.g., Quadrant II in Figure 6 and Quadrant III in Figure S3 in the supporting information). Mineralization of NDOM is also consistent with the negative ΔAlk (−41.6 ± 189.1 mg/L $CaCO_3$) and negative ΔpH (−0.1 ± 0.2) found for most of the samples in this quadrant (Table S4 in the supporting information).

Most of these samples were collected during low-flow periods, indicating that, although new NDOM may be supplied to some parts of the aquifer during high-flow conditions, the products of NDOM mineralization are only observed to build up during low flow. Deep well samples displayed greater production of DIC (ΔDIC = 24.3 ± 17.4 mg/L) and greater consumption of DOC (ΔDOC = −11.9 ± 9.7 mg/L) and DO (ΔDO = −2.7 ± 2.2 mg/L) relative to shallow well samples (21.0 ± 12.2 mg/L, −7.3 ± 4.9 mg/L, and 0.1 ± 2.5 mg/L, respectively). These findings suggest that NDOM mineralization proceeded to greater extents in deeper portions of the aquifer (especially at W2 and W7), which contradicts the idea that heterotrophic activities in karst aquifers are fueled primarily by labile OM imported from the surface [*Alberic and Lepiller*, 1998; *Hancock et al*., 2005; *Simon et al*., 2001]. It may be that the NDOM transported to the aquifer from the surface, though abundant, is more refractory than that generated by chemolithoautotrophy or released by carbonate dissolution. Alternatively, some of the greater delta values indicating more extensive mineralization in the deep aquifer could be explained by longer residence times of the water there. In any case, a few shallow well sites (e.g., W4a and W5a) did show greater mineralization during a very high-flow period showing that multiple sources of NDOM can fuel heterotrophic activity within a single karst aquifer.

5.5.3. Dissolution of Carbonate

Carbonate dissolution has been found previously in the Santa Fe River Sink-Rise system [*Martin and Dean*, 2001; *Moore et al*., 2010] as well as portions of other karst systems [e.g., *de Montety et al*., 2011; *Dreybrodt*, 1990; *Li et al*., 2010]. Many samples show evidence of carbonate dissolution in their negative ΔDIC values (Quadrant IV in Figure 6 and Quadrants I and IV in Figure S4 in the supporting information). Most of them also have positive ΔpH (0.3 ± 0.5) and ΔCa (46.9 ± 77.0 mg/L) values, as well as the negative $SI_{calcite}$ (−0.5 ± 0.9) and $SI_{dolomite}$ (−1.6 ± 1.8) (Table S4 in the supporting information). However, samples outside of Quadrant IV also show evidence of carbonate dissolution with positive ΔCa and ΔSpC and negative $SI_{calcite}$ and $SI_{dolomite}$, particularly those that fall into Quadrant II and those plotting near the origin of Figure 6 (Table S4 in the supporting information). Many of these samples were collected from deep wells (especially W4 and W6) and during low-flow conditions when water would have been expected to flow from the aquifer matrix into the conduits [*Martin and Dean*, 2001; *Moore et al*., 2009; *Screaton et al*., 2004]. Thus, although pervasive in the Sink-Rise system, carbonate dissolution tends to occur to greater extents or accumulate more concentrated products, in the deep portion of the aquifer and during low-flow conditions than in the shallow aquifer and during high-flow conditions.

In a study of cave enlargement in the Suwannee River in north Florida, *Gulley et al*. [2011] reported that carbonate dissolution occurs during flooding of the river, and this dissolution would occur at the contact between conduit walls and flood water during flow reversals when river water that is highly undersaturated with respect to carbonate minerals recharges the UFA. In this study, however, carbonate dissolution in the Sink-Rise system is found to be pervasive through space and time, including during low-flow periods. These findings are not in conflict however since the *Gulley et al*. [2011] study was focused on conduit walls, and this study examined a spatiotemporally larger system. In addition, we observed "hot spots" of dissolution, such as the enhanced carbonate dissolution in shallow wells (W4a and W5a) during extreme high flow as well as in deep wells such as W4 and W6 during low-flow conditions. The correspondence of enhanced NDOM supply from surface waters as well as deep autotrophic production, its mineralization, and associated carbonate dissolution suggests that carbonate dissolution may occur through mineralization of both autochthonous and allochthonous NDOM. NDOM mineralization has also been found to play an important part in carbonate rock weathering by *Li et al*. [2010] based on DIC concentrations, $\delta^{13}C_{DIC}$ signatures, and P_{CO2} in a typical karstic catchment in southwest China. This finding suggests that subsurface biogeochemical processes may be more important to the evolution of karst aquifer than previously recognized.

5.5.4. NDOM-Mineral Desorption

In general, NDOM-mineral desorption occurred in spatiotemporal patterns similar to carbonate dissolution providing evidence that carbonate dissolution and NDOM-mineral desorption are linked in this system. For example, samples in Quadrant I and those close to the origin of Figure 6 may reflect NDOM-mineral desorption, which resulted in the small, positive ΔDOC values calculated for most of these samples. Similarly, samples falling in Quadrant IV of Figure 6 may have also gained DOC via desorption of NDOM from carbonate rocks. This conclusion is supported by experimental observation of OM release during UFA rock dissolution [*Jin and Zimmerman*, 2010].

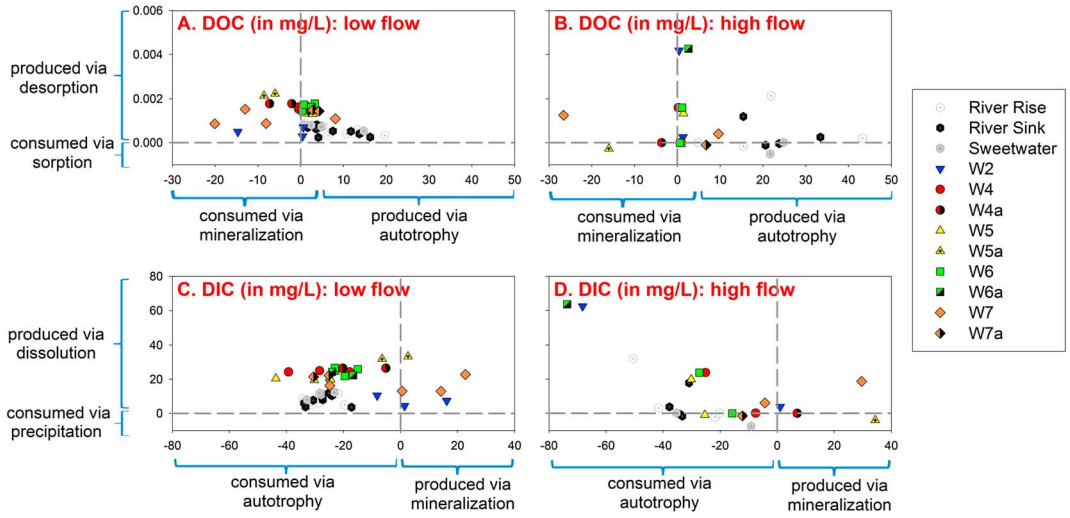

Figure 7. Calculated changes (in mg/L) in (a and b) DOC and (c and d) DIC in samples from the Sink-Rise system that can be ascribed to each biogeochemical process during low-flow condition in Figures 7a and 7c and high-flow condition in Figures 7b and 7d. See text for calculation method.

5.6. Relative Magnitudes of Biogeochemical Processes

The results of the model (Δ values) only provide information on the net effects of simultaneously occurring biogeochemical processes, each of which may have an additive or a subtractive effect on a particular solute concentration. Some sense of the relative magnitude of each of these biogeochemical processes may be had by assuming specific reaction stoichiometries and thus ratios of elements produced and consumed by each process. First, using ΔCa values, we estimate the amount of DIC to have been released or consumed via carbonate mineral dissolution or precipitation, respectively, using a DIC:Ca molar ratio of 1:1. This assumes the aquifer material in the study area to be stoichiometric calcite. Next, DOC consumed or released via NDOM-mineral sorption or desorption following carbonate dissolution or precipitation, respectively, was calculated by assuming a ratio of 8.0 mg DOC/kg rock (or a DOC:Ca molar ratio of 6.7×10^{-5}). This was based on triplicate desorption experiments using Floridan aquifer materials (300 g Suwannee Limestone rock, ground to 1 mm grain size, shaken 3 days in 1 L DI water, unpublished data but method details provided by *Jin and Zimmerman* [2010]). Lastly, changes in DIC and DOC attributable to mineralization/autotrophy were calculated as that portion of ΔDIC or ΔDOC as yet unaccounted for. These calculations can be expressed as

$$\Delta DIC_{dissolution/precipitation} = \Delta Ca \tag{9}$$

$$\Delta DIC_{autotrophy/respiration} = \Delta DIC_{total} - \Delta DIC_{dissolution/precipitation} \tag{10}$$

$$\Delta DOC_{desorb/sorb} = 6.7 \times 10^{-5} \times \Delta Ca \tag{11}$$

$$\Delta DOC_{autotrophy/respiration} = \Delta DOC_{total} - \Delta DOC_{desorb/sorb.} \tag{12}$$

These calculations show that DIC and DOC quantities in samples collected in the Sink-Rise system over the 6 year sampling period were influenced most strongly by autotrophy and carbonate dissolution (by a magnitude of tens of mg C/L: Figure 7). Nearly all surface water samples and about 1 quarter of well water samples indicated autotrophy to have altered DOC or DIC composition by >5 mg/L. The rates of autotrophic production of DOC in the surface water almost tripled when the hydrologic conditions shifted from low to high flow (7.2 ± 6.0 mg/L versus 22.8 ± 10.8 mg/L, on average, respectively), suggesting that the introduction of new nutrients stimulated photosynthesis. Addition of >5 mg/L DIC could be attributed to carbonate dissolution in 70% of the surface samples and 80% of the well water samples. The magnitude of DIC release via dissolution is clearly greater in groundwater versus surface waters, in shallow versus deep groundwater wells, and usually during low versus high-flow periods.

In contrast, no surface waters samples and only 22% of well water samples indicated DOC losses of >5 mg/L due to NDOM mineralization. The loss of NDOM via mineralization was greater at deep well sites (W2 and W7) during low-flow periods and shallow wells during extreme high flow (W4a and W5a) as was carbonate dissolution (W2, W6, and W5a) suggesting a possible linkage between NDOM mineralization and carbonate dissolution. These observations also suggest that heterotrophic activities in karst aquifers are not necessarily fueled primarily by labile OM imported from the surface. While NDOM-mineral desorption reactions were found to alter C concentrations in almost all the samples collected, they had an influence on DOC concentrations about 1000 times less than NDOM mineralization/production. Lastly, NDOM-mineral sorption and carbonate precipitation were rarer and, when present, had only small effects on DIC and DOC concentrations.

The interpretations made from the calculation results depicted in Figure 6 and those in Figure 7 are mutually supportive. Again, it is worth noting that the sensitivity analyses predicted the effects of model error on DIC and DOC biogeochemical shifts of <5 mg/L for any given sample. Shifts of this magnitude would be relatively small compared the chemical effects of biogeochemical processes shown in Figure 7.

6. Summary and Environmental Implications

Much of the spatiotemporal variations in organic and inorganic C concentrations observed in the Sink-Rise system during this study resulted from mixing of three water sources identified as originating from organic-rich soils or wetlands, from the shallow aquifer and from the deep aquifer. After taking into account the effects of mixing on each solute concentration, evidence for the occurrence of biogeochemical processes such as autotrophic production, NDOM mineralization, carbonate mineral dissolution, and NDOM-mineral desorption was found at different times and in different portions of the system. In general, surface waters in the Sink-Rise system could be characterized as net autotrophic, while the groundwater was often in close to metabolic balance (i.e., heterotrophic C consumption was similar to autotrophic C production). However, there were hot spots of enhanced heterotrophic activity such as in the shallow aquifer during high-flow periods and in the deep aquifer where chemolithoautotrophy was identified. The biogeochemical processes observed however are likely to be linked. For instance, both surface and deep autotrophic production fueled subsurface NDOM mineralization, which can render the water more acidic and drive carbonate dissolution. The dissolution of aquifer materials releases indigenous NDOM that may fuel further microbial respiration.

The findings of this study have a number of environmental implications. For instance, it is not necessarily true that the surface water injected into an aquifer during hydrogeologic operations such as aquifer storage and recovery and aquifer recharge will fuel heterotrophic microbial activity. Here, we find this NDOM to be too refractory or not widely enough distributed to result in large-scale changes in C cycling. To the contrary, it may be that these operations are of larger concern for the nutrients and electron acceptors they may carry to fuel subsurface autotrophic production. It is clear from this study that imported solutes may also result in dissolution of the karst aquifer through the biogeochemical processes they stimulate. Given the heterogeneity of the aquifer biogeochemistry, there may be preferential locations for these hydrogeologic operations to be carried out such as those carbonate formations with lower NDOM content or those lacking deep upwellings.

This study also shows that karst subsurface geomorphology can be modified not only via abiotic processes but also via linkages with various biogeochemical processes in which NDOM and microbes are certainly involved. Greater consideration of these processes should be made by those studying landscape, cave, and hydrological evolution within karst aquifers. The results of this study may also facilitate contaminant remediation operations in karst aquifer by advancing our knowledge of the subsurface biogeochemistry. For instance, this study sheds light on the possible mechanisms of secondary porosity development and subsurface NDOM production, both of which greatly influence the fate and transport of contaminants. Finally, the linked source water mixing model and biogeochemical calculations developed in this study show promise as a tool to evaluate C dynamic processes and their spatiotemporal distributions in complex surface-groundwater exchange systems such as karst regions.

Acknowledgments

We thank Jason Curtis for his assistance with the DIC and C isotope measurement and Elizabeth Screaton, Kathleen McKee, and Megan Wetherington for providing the hydrologic data. This work was funded by grants from the University of Florida Water Institute, Florida Department of Environmental Protection S0060, S0141, and S0181 and NSF EAR-0510054 and EAR-0853956.

References

Alberic, P., and M. Lepiller (1998), Oxidation of organic matter in a karstic hydrologic unit supplied through stream sinks (Loiret, France), *Water Res.*, *32*(7), 2051–2064.

Aravena, R., L. I. Wassenaar, and E. C. Spiker (2004), Chemical and carbon isotopic composition of dissolved organic carbon in a regional confined methanogenic aquifer, *Isot. Environ. Health Stud.*, *40*(2), 103–114.

Arthur, J. D., A. A. Dabous, and J. B. Cowart (2002), Mobilization of arsenic and other trace elements during aquifer storage and recovery, southwest Florida, paper presented at U.S. Geological Survey Artificial Recharge Workshop Proceedings, U.S. Geological Survey, Sacramento, Calif.

Batiot, C., C. Emblanch, and B. Blavoux (2003), Total Organic Carbon (TOC) and magnesium (Mg^{2+}): Two complementary tracers of residence time in karstic systems, *C. R. Geosci.*, *335*(2), 205–214.

Birdwell, J. E., and A. S. Engel (2009), Variability in terrestrial and microbial contributions to dissolved organic matter fluorescence in the Edwards Aquifer, central Texas, *J. Cave Karst Stud.*, *71*(2), 144–156.

Budd, D. A., and H. L. Vacher (2004), Matrix permeability of the confined Floridan Aquifer, Florida, USA, *Hydrogeol. J.*, *12*(5), 531–549.

Chapelle, F. H., P. M. Bradley, D. R. Lovley, K. O'Neill, and J. E. Landmeyer (2002), Rapid evolution of redox processes in a petroleum hydrocarbon-contaminated aquifer, *Ground Water*, *40*(4), 353–360.

Clark, I. D., and P. Fritz (1997), *Environmental Isotopes in Hydrogeology*, CRC Press, Boca Raton, Fla.

Davis, J. A. (1982), Adsorption of natural dissolved organic-matter at the oxide water interface, *Geochim. Cosmochim. Acta*, *46*(11), 2381–2393.

de Montety, V., J. B. Martin, M. J. Cohen, C. Foster, and M. J. Kurz (2011), Influence of diel biogeochemical cycles on carbonate equilibrium in a karst river, *Chem. Geol.*, *283*(1-2), 31–43.

Drever, J. I. (2002), *The Geochemistry of Natural Waters: Surface and Groundwater Environments*, pp. 114–116, Prentice Hall, Upper Saddle River, N. J.

Dreybrodt, W. (1990), The role of dissolution kinetics in the development of karst aquifers in limestone - a model simulation of karst evolution, *J. Geol.*, *98*(5), 639–655.

Engel, A. S., M. L. Porter, L. A. Stern, S. Quinlan, and P. C. Bennett (2004), Bacterial diversity and ecosystem function of filamentous microbial mats from aphotic (cave) sulfidic springs dominated by chemolithoautotrophic "Epsilonproteobacteria", *FEMS Microbiol. Ecol.*, *51*(1), 31–53.

Farnleitner, A. H., I. Wilhartitz, G. Ryzinska, A. K. Kirschner, H. Stadler, M. M. Burtscher, R. Hornek, U. Szewzyk, G. Herndl, and R. L. Mach (2005), Bacterial dynamics in spring water of alpine karst aquifers indicates the presence of stable autochthonous microbial endokarst communities, *Environ. Microbiol.*, *7*(8), 1248–1259.

Findlay, S. E. G., and R. L. Sinsabaugh (2003), *Aquatic Ecosystems: Interactivity of Dissolved Organic Matter*, 1st ed., Academic Press, Amsterdam, The Netherlands.

Florea, L. J., and H. L. Vacher (2006), Springflow hydrographs: Eogenetic vs. telogenetic karst, *Ground Water*, *44*(3), 352–361.

Ford, D. C., and P. W. Williams (2007), *Karst Hydrogeology and Geomorphology*, pp. 562, Wiley, Chichester, U. K.

Frimmel, F. H. (1998), Characterization of natural organic matter as major constituents in aquatic systems, *J. Contam. Hydrol.*, *35*(1-3), 201–216.

Frye, G. C., and M. M. Thomas (1993), Adsorption of organic-compounds on carbonate minerals. 2. Extraction of carboxylic-acids from recent and ancient carbonates, *Chem. Geol.*, *109*(1-4), 215–226.

Grubbs, J. W. (1998), Recharge rates to the Upper Floridan Aquifer in the Suwannee River Water Management District, Florida, *U. S. Geol. Surv. Water Resour. Invest. Rep.*, *97-4283*, 30.

Gulley, J., J. B. Martin, E. J. Screaton, and P. J. Moore (2011), River reversals into karst springs: A model for cave enlargement in eogenetic karst aquifers, *Geol. Soc. Am. Bull.*, *123*(3-4), 457–467.

Hancock, P. J., A. J. Boulton, and W. F. Humphreys (2005), Aquifers and hyporheic zones: Towards an ecological understanding of groundwater, *Hydrogeol. J.*, *13*(1), 98–111.

Haque, S. E., J. Tang, W. J. Bounds, D. J. Burdige, and K. H. Johannesson (2007), Arsenic geochemistry of the great dismal swamp, Virginia, USA: Possible organic matter controls, *Aquat. Geochem.*, *13*(4), 289–308.

Heffernan, J. B., M. J. Cohen, T. K. Frazer, R. G. Thomas, T. J. Rayfield, J. Gulley, J. B. Martin, J. J. Delfino, and W. D. Graham (2010), Hydrologic and biotic influences on nitrate removal in a subtropical spring-fed river, *Limnol. Oceanogr.*, *55*(1), 249–263.

Hoch, A. R., M. M. Reddy, and G. R. Aiken (2000), Calcite crystal growth inhibition by humic substances with emphasis on hydrophobic acids from the Florida Everglades, *Geochim. Cosmochim. Acta*, *64*(1), 61–72.

Hoffer-French, K. J., and J. S. Herman (1989), Evaluation of hydrological and biological influences on CO_2 fluxes from a karst stream, *J. Hydrol.*, *108*(1-4), 189–212.

Inskeep, W. P., and P. R. Bloom (1986), Kinetics of calcite precipitation in the presence of water-soluble organic-ligands, *Soil Sci. Soc. Am. J.*, *50*(5), 1167–1172.

Jiang, J., and A. Kappler (2008), Kinetics of microbial and chemical reduction of humic substances: Implications for electron shuttling, *Environ. Sci. Technol.*, *42*(10), 3563–3569.

Jin, J., (2012), Natural dissolved organic matter dynamics in a karstic surface-groundwater exchange system, PhD dissertation, 168 pp., University of Florida, Gainesville, Fla.

Jin, J., and A. R. Zimmerman (2010), Abiotic interactions of natural dissolved organic matter and carbonate aquifer rock, *Appl. Geochem.*, *25*(3), 472–484.

Konhauser, K. (2007), *Introduction to Geomicrobiology*, Blackwell Publishing, Oxford, U. K.

Kurz, R. C., et al. (2004), *Mapping and Monitoring Submerged Aquatic Vegetation in Ichetucknee Springs*, pp. 135, Suwanee River Water Management District, Live Oak, Fla.

Langston, A. L., E. J. Screaton, J. B. Martin, and V. Bailly-Comte (2012), Interactions of diffuse and focused allogenic recharge in an eogenetic karst aquifer (Florida, USA), *Hydrogeol. J.*, *20*(4), 767–781.

Lau, L. S., and J. F. Mink (1987), Organic contamination of groundwater - A learning-experience, *J. Am. Water Works Assn.*, *79*(8), 37–42.

Lee, E. S., and N. C. Krothe (2001), A four-component mixing model for water in a karst terrain in south-central Indiana, USA. Using solute concentration and stable isotopes as tracers, *Chem. Geol.*, *179*(1-4), 129–143.

Lee, J. U., S. W. Lee, K. W. Kim, and C. H. Yoon (2005), The effects of different carbon sources on microbial mediation of arsenic in arsenic-contaminated sediment, *Environ. Geochem. Health*, *27*(2), 159–168.

Li, S.-L., C.-Q. Liu, J. Li, Y.-C. Lang, H. Ding, and L. Li (2010), Geochemistry of dissolved inorganic carbon and carbonate weathering in a small typical karstic catchment of Southwest China: Isotopic and chemical constraints, *Chem. Geol.*, *277*(3-4), 301–309.

Lin, Y. P., and P. C. Singer (2005), Inhibition of calcite crystal growth by polyphosphates, *Water Res.*, *39*(19), 4835–4843.

Lindroos, A. J., V. Kitunen, J. Derome, and H. S. Helmisaari (2002), Changes in dissolved organic carbon during artificial recharge of groundwater in a forested esker in Southern Finland, *Water Res.*, *36*(20), 4951–4958.
Lovley, D. R., and F. H. Chapelle (1995), Deep subsurface microbial processes, *Rev. Geophys.*, *33*(3), 365–381.
Martin, J. B., and R. W. Dean (2001), Exchange of water between conduits and matrix in the Floridan aquifer, *Chem. Geol.*, *179*, 145–165.
Martin, J. B., and P. J. Moore (2007), Hydrogeology of O'Leno State Park and Nitrate Loading from the River Rise, A First Magnitude Spring. Comprehensive Project Report. DEP Agreement S0182.
McCarthy, J. F., B. Gu, L. Liang, J. Mas-Pla, T. M. Williams, and T.-C. J. Yeh (1996), Field tracer tests on the mobility of natural organic matter in a sandy aquifer, *Water Resour. Res.*, *32*(5), 1223–1238.
Miller, J. A. (1986), Hydrogeologic Framework of the Floridan Aquifer System in Florida and in Parts of Georgia, Alabama, and South Carolina, *US Geological Survey Professional Paper 1403-B*.
Moore, P. J., J. B. Martin, and E. J. Screaton (2009), Geochemical and statistical evidence of recharge, mixing, and controls on spring discharge in an eogenetic karst aquifer, *J. Hydrol.*, *376*(3-4), 443–455.
Moore, P. J., J. B. Martin, E. J. Screaton, and P. S. Neuhoff (2010), Conduit enlargement in an eogenetic karst aquifer, *J. Hydrol.*, *393*, 143–155.
Opsahl, S. P., and J. P. Chanton (2006), Isotopic evidence for methane-based chemosynthesis in the Upper Floridan aquifer food web, *Oecologia*, *150*(1), 89–96.
Pabich, W. J., I. Valiela, and H. F. Hemond (2001), Relationship between DOC concentration and vadose zone thickness and depth below water table in groundwater of Cape Cod, USA, *Biogeosciences*, *55*(3), 247–268.
Pavelic, P., B. C. Nicholson, P. J. Dillon, and K. E. Barry (2005), Fate of disinfection by-products in groundwater during aquifer storage and recovery with reclaimed water, *J. Contam. Hydrol.*, *77*(1-2), 119–141.
Petrovic, M., M. Kaštelan-macan, and A. J. M. Horvat (1999), Interactive sorption of metal ions and humic acids onto mineral particles, *Water Air Soil Pollut.*, *111*(1-4), 41–56.
Randazzo, A. F., and D. S. Jones (1997), *The Geology of Florida*, University Press of Florida, Gainesville, Fla.
Ratasuk, N., and M. A. Nanny (2007), Characterization and quantification of reversible redox sites in humic substances, *Environ. Sci. Technol.*, *41*, 7844–7850.
Rauch, T., and L. Drewes (2004), Assessing the removal potential of soil-aquifer treatment systems for bulk organic matter, *Water Sci. Technol.*, *50*(2), 245–253.
Ritorto, M., E. J. Screaton, J. B. Martin, and P. J. Moore (2009), Relative importance and chemical effects of diffuse and focused recharge in an eogenetic karst aquifer: An example from the unconfined upper Floridan aquifer, USA, *Hydrogeol. J.*, *17*(7), 1687–1698.
Sarbu, S. M., T. C. Kane, and B. K. Kinkle (1996), A chemoautotrophically based cave ecosystem, *Science*, *272*(5270), 1953–1955.
Schlautman, M. A., and J. J. Morgan (1994), Adsorption of aquatic humic substances on colloidal-size aluminum-oxide particles - Influence of solution chemistry, *Geochim. Cosmochim. Acta*, *58*(20), 4293–4303.
Schwarzenbach, R. P., P. M. Gschwend, and D. M. Imboden (2003), *Environmental Organic Chemistry*, 2nd ed., pp. 280-283, Wiley-Interscience, New York.
Screaton, E., J. B. Martin, B. Ginn, and L. Smith (2004), Conduit properties and karstification in the unconfined Floridan Aquifer, *Ground Water*, *42*(3), 338–346.
Simon, K. S., J. Gibert, P. Petitot, and R. Laurent (2001), Spatial and temporal patterns of bacterial density and metabolic activity in a karst aquifer, *Arch. Hydrobiol.*, *151*(1), 67–82.
Thomas, M. M., J. A. Clouse, and J. M. Longo (1993), Adsorption of organic-compounds on carbonate minerals. 3. Influence on dissolution rates, *Chem. Geol.*, *109*(1-4), 227–237.
USEPA (1983), *Methods for the Chemical Analysis of Water and Wastes*, pp. 552, Office of Research and Development, US Environmental Protection Agency, Cincinnati, Ohio.
Vacher, H. L., and J. E. Mylroie (2002), Eogenetic karst from the perspective of an equivalent porous medium, *Carbonates Evaporates*, *17*(2), 182–196.
Vlasceanu, L., S. M. Sarbu, A. S. Engel, and B. K. Kinkle (2000), Acidic cave-wall biofilms located in the Frasassi Gorge, Italy, *Geomicrobiol. J.*, *17*(2), 125-139.
Worthington, S. R. H. (1994), Flow velocities in unconfined carbonate aquifers, *Cave Karst Sci.*, *21*, 21–22.
Wu, Y. (2003), Mechanism analysis of hazards caused by the interaction between groundwater and geo-environment, *Environ. Geol.*, *44*(7), 811–819.
Wu, Y. T., and C. Grant (2002), Effect of chelation chemistry of sodium polyaspartate on the dissolution of calcite, *Langmuir*, *18*(18), 6813–6820.